Facultad de **Medicina**

GRADO EN CIENCIAS BIOMÉDICAS

TRABAJO FIN DE GRADO

Escribir Título TFG en Castellano

Modelado *in vitro* del envejecimiento mediante epitelioides 3D a largo plazo

Escribir Título TFG en Inglés

In vitro modelling of aging using long-term 3D Epithelioids

Autor/a: Naiara Martínez Melgosa

Director/es: David Fernández Antorán

Alberto Pradilla Dieste

Santander, 8 de junio **20**25

Table of contents

Trabajo de Fin de Grado
Grado en Ciencias Biomédicas · Facultad de Medicina
2024 – 2025

In vitro modelling of ageing using long-term 3D epithelioids

GRAPHICAL ABSTRACT

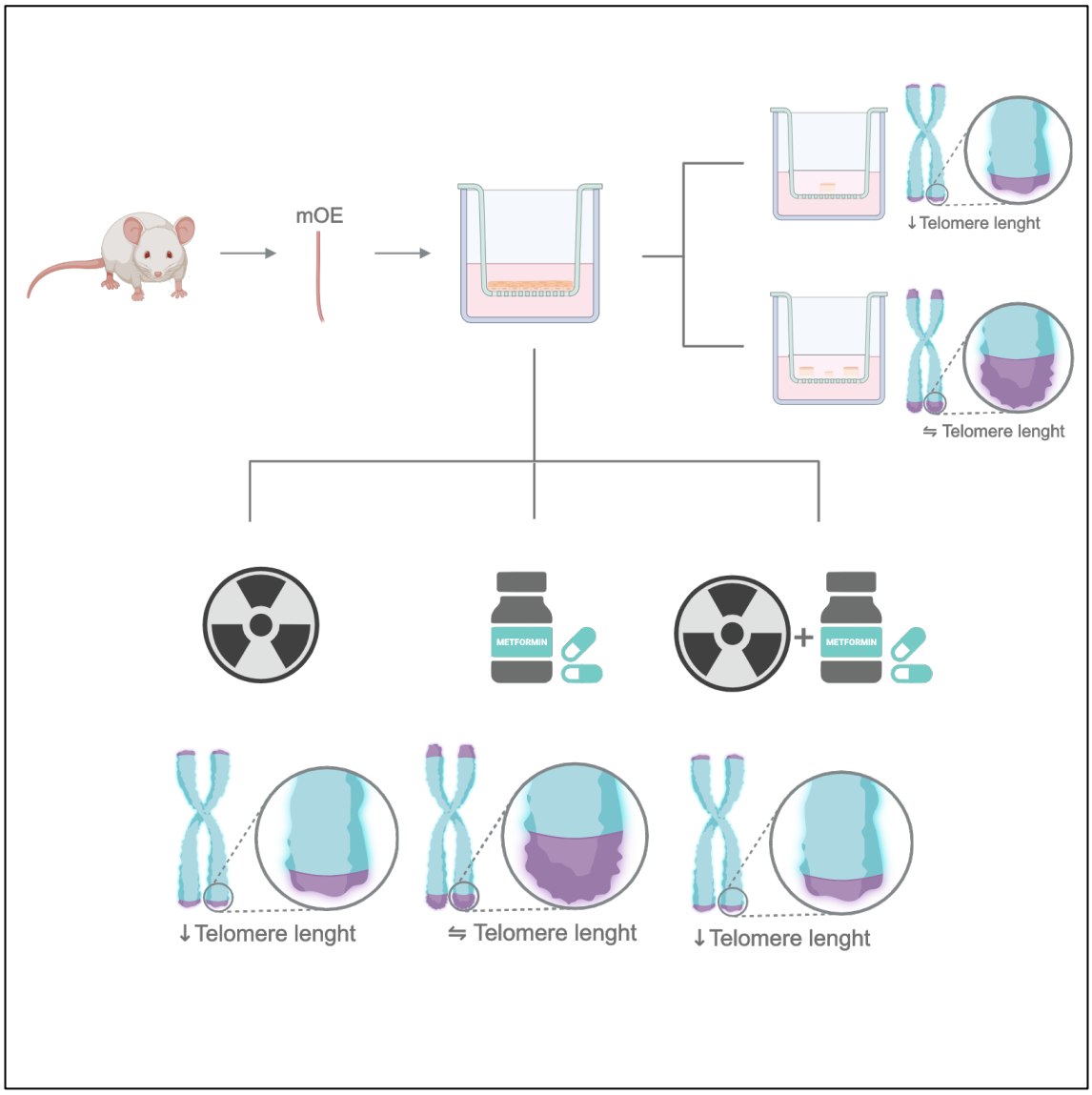

AUTHORS

Naiara Martínez Melgosa, Alberto Pradilla Dieste, David Fernández-Antorán.

Correspondencia: df336@cam.ac.uk

UC | Universidad de Cantabria

In vitro modelling of ageing using long-term 3D epithelioids

Naiara Martínez Melgosa[1,2], Alberto Pradilla Dieste[2] David Fernández-Antorán[2,3]

[1]Universidad de Cantabria, Santander, Spain
[2]Gurdon Institute- University of Cambridge, Cambrige, UK
[3]ARAID-IIS-Aragon, Zaragoza, Spain

* Correspondencia: df336@cam.ac.uk

RESUMEN

Uno de los principales “hallmarks” del envejecimiento es el acortamiento de telómeros, que se puede correlacionar con la esperanza de vida de los organismos y puede estar influenciada por factores internos y externos, que afectan en última instancia al proceso de envejecimiento. En el presente estudio se demuestra que la longitud de los telómeros puede ser medida en epitelioides generados a partir de esófago, cultivos en 3D a largo plazo. Los epitelioides recapitulan *in vitro* la arquitectura y las propiedades mecánicas de los tejidos epiteliales. Los epitelioides han sido expuestos a factores externos, que modulan la longitud de los telómeros y han sido medidos sus correspondientes variaciones. Nuestros resultados muestran que una exposición a baja dosis de radiación ionizante induce acortamiento en los telómeros, mientras que el tratamiento con metformina mantiene la longitud original de los mismos a lo largo del tiempo. Estos descubrimientos destacan la robustez y relevancia de los epitelioides como un modelo para estudiar las dinámicas de los telómeros, así como los procesos relacionados con el envejecimiento.

ABSTRACT

One of the hallmarks of ageing is telomere shortening, which has been closely correlated with organismal lifespan and can be influenced by various external and internal factors, ultimately affecting the ageing process. In this study, we demonstrate that telomere length can be reliably measured in long-term 3D epithelioid oesophageal cultures. Epithelioids recapitulate the architecture and mechanical properties of epithelial tissues in vivo, offering a more physiologically relevant in vitro model. We exposed epithelioids to different external factors known to modulate telomere length and measured corresponding changes. Our results show that exposure to low doses of ionizing radiation leads to telomere shortening whereas treatment with metformin seems to preserve telomere length over time. These findings highlight the robustness and relevance of the epithelioids as a platform for studying telomere dynamics and ageing-related processes.

KEY WORDS

Ageing, telomere shortening, senescence, epithelioids, oesophagus, 3D cultures, long-term, radiation, metformin.

INTRODUCTION

Ageing is defined as the irreversible, time-dependent loss of physiological integrity and function caused by a series of interrelated statements called hallmarks that collectively form the basis of this complex process. This functional decline over time makes people more vulnerable to age-related illnesses such cancer, musculoskeletal conditions like arthritis, cardiovascular diseases, and neurological diseases[1,2].

There is evidence supporting the role of telomere shortening in the induction of replicative senescence. As cells approach replicative senescence, they experiment a gradual increase in cell size and duration of cell cycle that can be linked to the process of telomere shortening[3]. Telomeres are the chromosomal-end tracts, and they consist of tandemly repeated DNA sequences that are highly regulated and dynamic flanked by associated protective proteins[4]. As cellular division occurs, cells experience telomere attrition, where those protective caps are gradually shortening due to replicative DNA polymerases being unable to complete the copy of telomere regions in eukaryotic DNA. This fact contributes to genomic instability and cellular aging[5]. These effects on telomeres can be mitigated by telomerase, a ribonucleoprotein DNA polymerase that can elongate telomeres by addition of TTAGGG repeats onto the chromosome ends[2,6].

The telomere shortening rate of a species can be used to predict the life span of that species. In this regard, some studies correlate DNA repair ability to species longevity[7]. Mice with hyper-long telomeres had an increased longevity and develop less tumors associated with ageing. Those findings provided evidence that longer telomeres confer beneficial effects in mice, delaying metabolic ageing and cancer, resulting in longer lifespans[6].

In summary, telomere shortening is considered one of the hallmarks of aging as short telomeres are sufficient to cause organismal aging and decreased lifespan[6].

Accumulation of senescent cells is one of the hallmarks of ageing[1]. This may contribute to the development of the disorders previously mentioned[5]. Cell cycle is a highly plastic process wherein cells can follow different pathways en route to cell division or cell cycle arrest[8]. Cellular senescence is a state of irreversible cell-cycle arrest, during which cells develop a complex senescence-associated secretory phenotype (SASP), that includes alterations in cellular morphology and genetics[9]. p21 is identified as a key player in senescence phenotype caused by telomere attrition. High levels of p21 inhibit the cyclin D1-CDK4 complex, resulting in cell cycle arrest, whereas lower levels of p21 promote the activation of cyclin D1-CDK4 complex, thereby facilitating cell proliferation[10].

Other damage-causing agents, such as genetics and environmental factors can also contribute to telomere-shortening processes and ageing[4,9]. One environmental factor that can influence cellular ageing is radiation. There is evidence that high doses of radiation induce activation of ageing-related mechanisms, but the effect of low doses of radiation remains unclear[11]. Low dose ionizing radiation induces basal cell differentiation followed by increased compensatory proliferation. Mechanistically, it causes redox stress that acts as selective pressure by driving wild type cells to differentiate[12].

Aging has cellular processes associated as primary biological responses. This includes metabolic and inflammatory pathways. In this regard, metformin has shown effects on these aging-related mechanisms. It has positive prevention and treatment effects on ageing-related disease. Since it decreases levels of insulin, metformin has been normally

used to treat type 2 diabetes[1]. However, it might be a useful drug as a potential anti-ageing drug since its mechanism of action involves activating AMP-activating kinase (AMPK). This is supported by the claim that sensitivity to AMPK declines with age, so activators of AMPK may be helpful in this regard[13]. Metformin can decelerate ageing clock in male monkeys, proving that extended administration can act as a geroprotective drug in these organisms, not only physically, but also at the molecular level. Transcriptional profiles showed alterations related with inflammation and tissue regeneration (both hallmarks of ageing), after administration of metformin. Hepatoprotection and neuroprotection are other beneficial effects seen in primates after metformin administration[14].

To understand the cellular processes and the effects of environmental and other external factors, numerous types of cell cultures have been developed over the years.

In 2D cultures cells grow in monolayers, which allows uniform access to nutrients and growth factors present in the medium, resulting in homogenous growth and proliferation. However, the simplicity of these cell culture systems limits the replication of physiological environment *in vivo* in the cell culture development process[15]. As cells grow in monolayers, all cells receive the same amount of nutrients and growth factors from the medium and cells rarely differentiate. Although the requirements of these systems are easier to implement, some experiments such as drugs experiments are harder to assess since drugs are not well metabolized in 2D cultures. The representation of the response to mechanical stimuli of cells is also inaccurate[16].

The introduction of 3D cell culture has opened new possibilities to study the biochemical and biomechanical signals, thus enabling the reproduction of *in vivo* interactions[15]. Epithelial 3D cultures have allowed the study of multiple biological processes, such as epithelial cell proliferation, differentiation, motility, stress response, and both homotypic and heterotypic cell–cell communication. These systems can be experimentally manipulated, leading to a better understanding of the molecular mechanisms and signaling pathways underlying physiology and pathophysiology[17].

Advances in 3D culturing methods required more complex systems to allow different models to better recapitulate *in vivo* features. Extracellular matrix (ECM) components arose as essential for self-organization of functional epithelial cells in advanced 3D epithelial cultures[17]. Collagen coating or Matrigel embedding are two of the most commonly used compounds to mimic ECM[17]. Decellularized organs preserve native extracellular-matrix (ECM), overall architecture and composition and they can be used as natural scaffolds for cell anchorage, migration, growth, and 3D organization *in vitro*[18]. Organotypic 3D cultures (OTC) add an extra layer of complexity, growing epithelial cells over a collagen matrix containing fibroblasts that can mimic the lamina propria[17]. OTCs offer some advantages, including the ability to maintain normal polarization and differentiation patterns of cells, the gene signatures and the expression of genes involved in cell-cell adhesion[19]. Recent advances in biomaterial engineering led to the development of stable biocompatible formulations that can control key cellular processes such as stem cell differentiation in a cheap and simple way.

Another category of 3D cultures are spherical 3D structures of epithelial cells. This includes multicellular spheroids and organoids. Organoids are a unique type of culture highly similar to actual human that mimic human development or organ regeneration *in vitro*. They are 3D systems self-organized and they are generated from pluripotent stem cells or adult stem cells. Generation of spherical cultures usually requires a single

cell suspension or a small number of cells (less than 100) that are cultured under free-floating conditions, avoiding cells adhesion to a solid surface It has been demonstrated by spheroid culture of MSCs that intercellular interactions and differentiation can be recapitulated with this type of cultures[17,20,21]. 3D organoids can be generated with the same method. It is also possible to create secondary 3D organoids by passaging dissociated primary structures[17]. The potential of organoids has been developed as a good model to complement other existing models to extend basic biological research into a more physiologically relevant human setting, holding great potential in clinical translational research[21].

All these systems have limitations. They normally fail to reconstitute the tumor microenvironment (TME) because of the lack of stromal cells. Immune microenvironment could be modelled in organoids[22] but only for short-term modelling, fibroblasts and immune cells progressively decline over a month period. Furthermore, presence of Matrigel and the enriched growth factors surrounding the organoids can affect functional/morphological/biochemically and complicate the cell harvesting. Cost for organoids production is higher, generating and maintaining 3D culture systems is not as east as cell lines[23].

Epithelioids is one of the most recent examples of the effort for developing more complex *in vitro* 3D models that resemble *in vivo* tissues. Epithelioids are generated using small pieces of epithelial tissues plated on top of permeable membranes. Cells migrate from the explants and proliferate to cover the whole surface of the membrane. Once confluent, cultures differentiate and became mature, maintaining natural tissue architecture and also its dynamical and mechanical properties. This culture has a high potential in amplification of source tissue, since small explants can give rise to an expanded culture surface. Epithelioids are also defined as self-maintained, cells within the culture produce most of the factors that are needed for maintenance of the culture, reducing the factors that medium requires, and hence reducing medium complexity and associated costs. The most remarkable advantages from epithelioids are that they can be cultured for long-term (several months) in a continuous way (no need of trypsinization), conferring this system with a great potential to be used in studies involving ageing, cell competition or clonal evolution[24].

In the present study, the main goal is to deepen in the potential of long-term 3D epithelioids as a good model to be use for study aging.

RESULTS

Generation and characterization of mouse oesophageal epithelioids.

Current available advanced 3D cultures lack specific features that made them suitable for long-term ageing experiments. To overpass those limitations, mouse oesophageal epithelioids were the selected model due to their extended lifespan in comparison to other complex cultures systems.

Mouse oesophageal epithelioids were generated by plating mouse oesophagus explants on top of a permeable membrane (Figure 1A). Cultures were fed with cFAD until confluence and then media was changed to mFAD. To assess epithelioids structure and viability, cultures were maintained for two months after confluence. At this time point epithelioids are fully developed and mature. To facilitate staining and imaging steps, 5mm punches were collected from the whole membrane.

Different sets of staining were designed for characterization of mouse oesophageal epithelioids after two months in culture. First, polarity of epithelioids were characterized by two different markers, ITGα6 and KRT4. Itgα6 expression staining was restricted to basal cells (Figure 1B and 1D), while KRT4 strongly labeled cytoplasms in suprabasal cells (Figure 1B and 1C). Recapitulation of polarity in epithelioids was compared to those present in mouse oesophagus epithelium *in vivo*. ITGα6 and KRT4 expression pattern found in epithelioids correlated with the one showed in sections from mouse oesophagus (Figure S1A and S1B).

Regarding compartmentalization of the tissue, the second set of stainings consisted of Actin, KRT13 and Ki67. Actin expression pattern differed from basal and suprabasal. 2.5 months-old epithelioids showed a densely packed basal layer with small cells. On the other hand, suprabasal cells presented lower density, enlarged cytoplasm and a more intense actin staining (Figure 1C, 1F and 1I). Proliferation is confined only to basal cell, since Ki67 staining appeared only in this stratum (Figure 1E, 1F and 1G). Finally, KRT13 expression was restricted to suprabasal cells (Figure 1E, 1F and 1G). Compartmentalization in epithelioids replicated the one that can be found in mouse oesophageal epithelium (Figure S1C and S1D).

Finally, dynamics were assessed by expression of Loricrin and KLF4. Actin staining was included for structural purposes. Klf4 defines cells committed to differentiation in oesophageal epithelium, as shown in Figure S1F. Expression of KLF4 in epithelioids followed the same pattern as *in vivo* (Figure 1 H, 1I, 1J, S1E and S1F). Loricrin, as a terminal differentiation marker of keratinocytes was only expressed in the most external layer of the epithelioid (Figure 1H, 1I and 1J). Loricrin expression in epithelioids recapitulates the *in vivo* situation (Figure S1E and S1F).

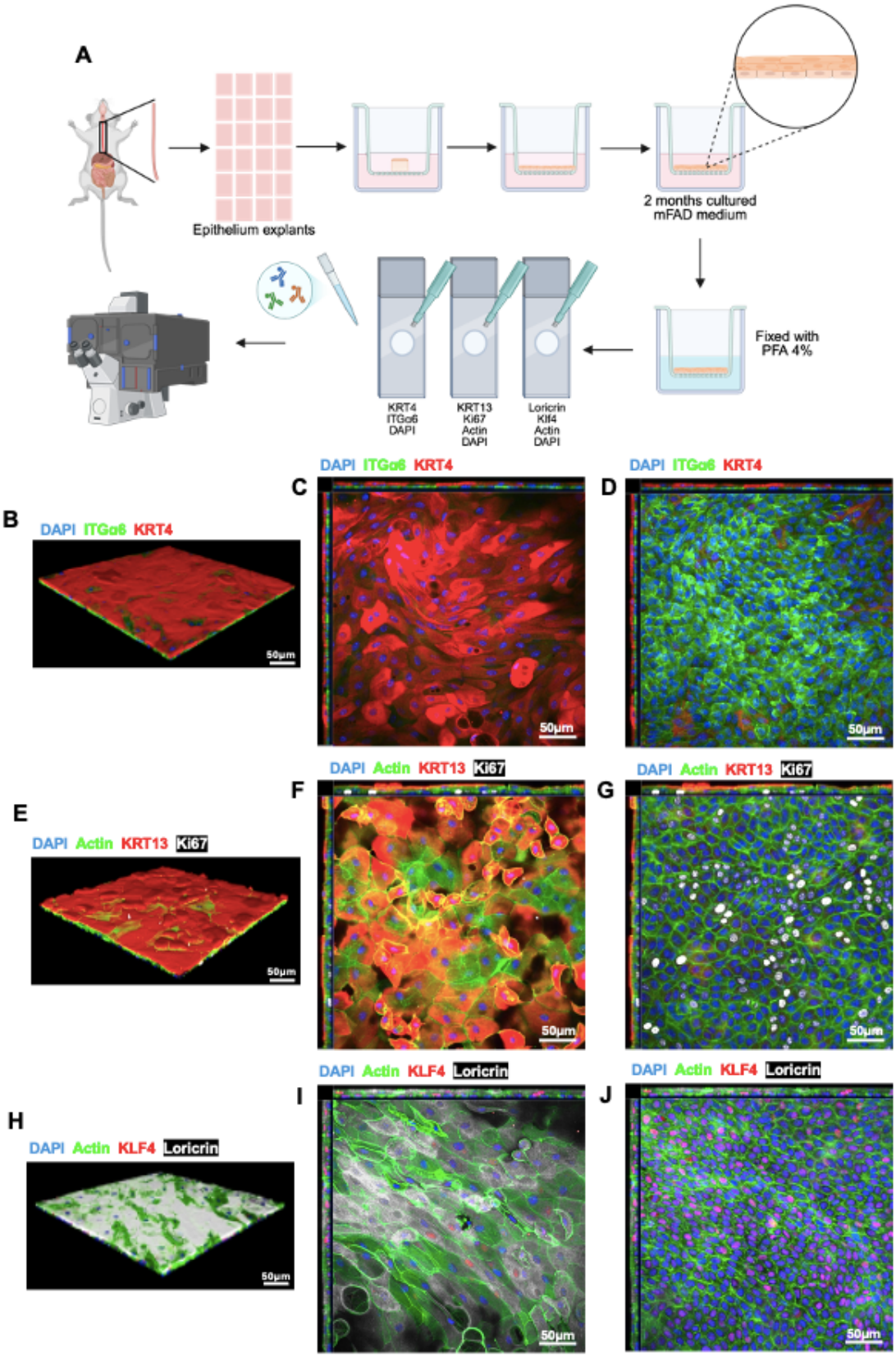
A
Epithelium explants
2 months cultured
mFAD medium
Fixed with
PFA 4%
KRT4
ITGα6
DAPI
KRT13
Ki67
Actin
DAPI
Loricrin
KII4
Actin
DAPI
B
DAPI ITGα6 KRT4
C
DAPI ITGα6 KRT4
D
DAPI ITGα6 KRT4
E
DAPI Actin KRT13 Ki67
F
DAPI Actin KRT13 Ki67
G
DAPI Actin KRT13 Ki67
H
DAPI Actin KLF4 Loricrin
I
DAPI Actin KLF4 Loricrin
J
DAPI Actin KLF4 Loricrin
50µm

Figure 1. Characterization of mouse oesophageal epithelioids.

(A) Generation of epithelioids protocol. **(B)** 3D rendered confocal z-stack stained for DAPI (blue), ITGα6 (green) and KRT4 (red). **(C)** Suprabasal layer optical section with orthogonal views. **(D)** Basal layer optical section with orthogonal views. **(E)** 3D rendered confocal z-stack stained for DAPI (blue), Actin (green), KRT13 (red) and Ki67 (white). **(F)** Suprabasal layer optical section with orthogonal views. **(G)** Basal layer optical section with orthogonal views. **(H)** 3D rendered confocal z-stack stained for DAPI (blue), Actin (green), KLF4 (red) and Loricrin (white). **(I)** Suprabasal layer optical section with orthogonal views. **(J)** Basal layer optical section with orthogonal views. Schematic cartoon was made using BioRender.

Effect of external factors in cellular ageing: radiation and metformin.

After characterizing mouse oesophageal epithelioids long-term capabilities (2.5 months), the next step was to assess how this novel 3D culture could be a valuable tool for ageing studies. As telomere shortening is one of the principal hallmarks of ageing, effects of external factors leading to telomere aging were tested in epithelioids for 6 weeks. The selected technique was an adapted version of quantitative FISH for labeling C-rich repetitions in the end section of the telomeres[25].

Epithelioids were treated with Irradiation (IR), Metformin (Met) or the combination (IR+Met) following the regime shown in Figure 2A.

During the exposition to IR and Met for 6 weeks, the cultures showed visual differences under the optical microscope. Control and Met-treated cultures were more homogeneous, with attached suprabasal cells (Figure 2B and 2D). IR treated culture showed more shedding cells detaching from the culture (Figure 2C). IR+Met treated cultures also looked homogeneous but with an increased in the number of shedding cells when compared to control.

Exposition to radiation showed a tendency in telomere shortening (less intensity) than control groups (Figure 2F). On the other hand, comparison between controls and those epithelioids treated with Metformin showed the same tendency in telomere length maintenance (more intensity).

Generation of epithelioids require that cells undergo several rounds of proliferation. To assess how this replicative pressure may affect culture outcomes, telomere length was also analyzed in cultures whose generation differed in the number of explants plates. For this experiment, two different approaches were used for generation of epithelioids (Figure S2A), one explant in the center of the insert (whose cells ended up covering the whole membrane, or three explants plated in the same way as described in the *Methods* section. Epithelioids were fixed when the culture reached confluence. FISH results showed a red dotty pattern in the nuclei of the basal cell (Figure S2B and S2C). Signal intensity is higher in nuclei from epithelioids generated from 3 explants (Figure S2C) than 1 explant (Figure S2B). There is a tendency showing that cultures generated using 3 explants have longer telomeres than those generated using only one explant (Figure S2D).

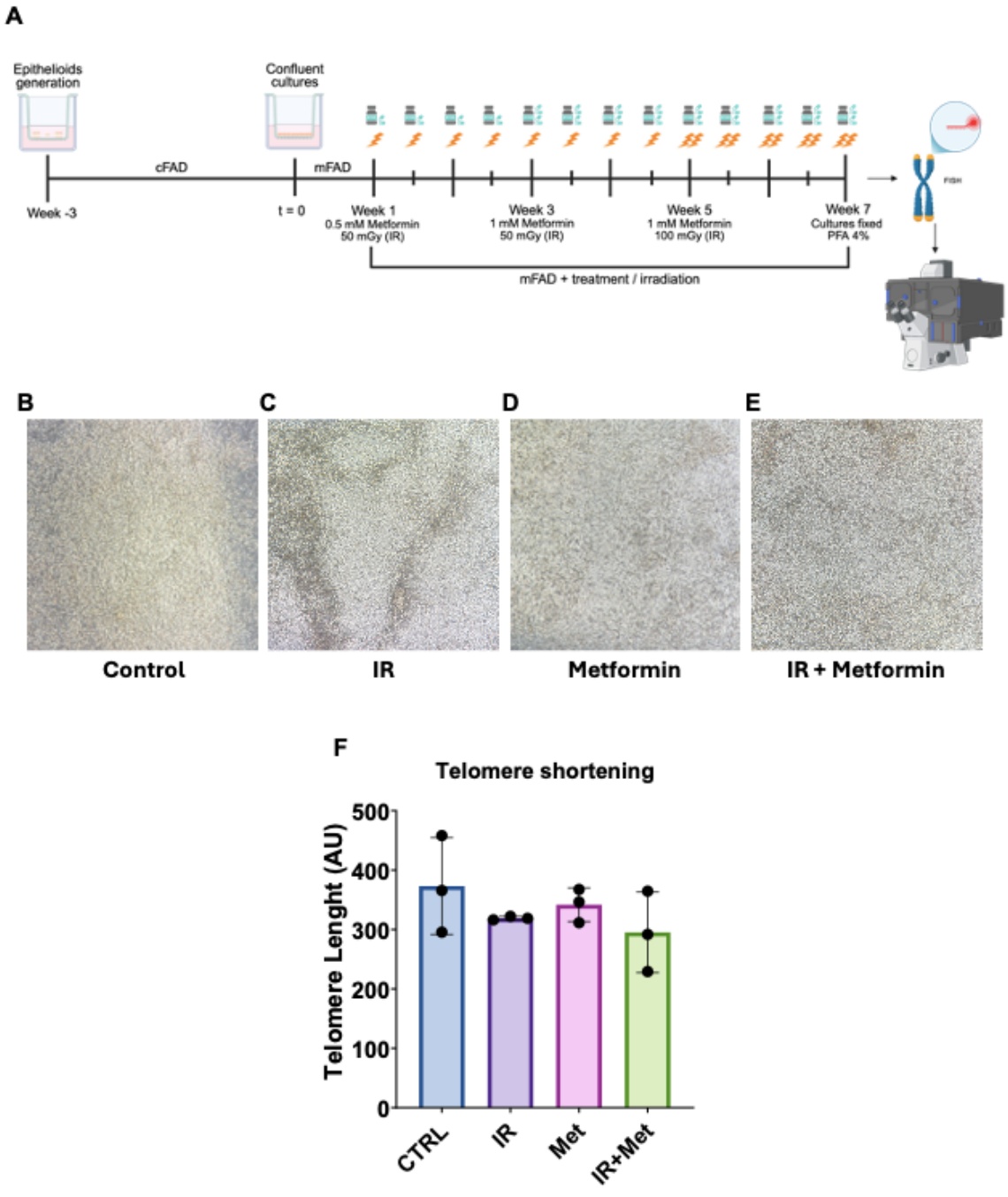

Figure 2. Differences in mouse oesophageal cultures exposed to external factors.

(A) Timeline of the experimental procedure (BioRender) **(B-E)** Representative images from epithelioids generated from mouse oesophagus epithelium. After 3 weeks of treatment using a light microscope (10x objective lens). **(F)** Graph showing the differences between the four groups exposed to the different combinations of external factors. Y-axis represents the average of telomere length in intensity arbitrary units (AU). Bars represent the mean of the intensity on each group. Chosen statistical analysis was Ordinary one-way ANOVA. N=3 different animals.

EdU allows tracing of differentiating cells in mouse oesophageal epithelioids.

5-ethynil 2´-deoxyuridine (EdU) is a thymidine analogue that proliferative cells in S-phase can intercalate in their DNA. However, EdU can be also used for tracking differentiation, since epithelial cells that undergo proliferation will be detached from the basal membrane and migrate upwards. EdU positive cells in upper layers of the epithelioid can be used to measure differentiation (Figure 3A). Cultures were incubated with EdU for one hour, then irradiated and kept in fresh mFAD for 24 hours to allow cells to differentiate.

Figures 3B-E correspond with representative images from the suprabasal layer of the epithelioids. Suprabasal layer in all four different conditions showed EdU+ cells in red color. Cells uptaked EdU during incubation time and then divided during the 24-hour chase, sharing EdU-labeled DNA with daughter cells (Figure 3A). Differentiation can be appreciated in Figures 3B-E, where red cells are the daughter cells divided from the basal ones that captured EdU.

Cell density was quantified from mouse oesophageal epithelioids. DAPI stained nuclei were counted and then calculated the number of cells per mm^2. Figure S3 shows a graph where there is a tendency showing that the radiation-exposed group compared present lower cell density compared to the other groups.

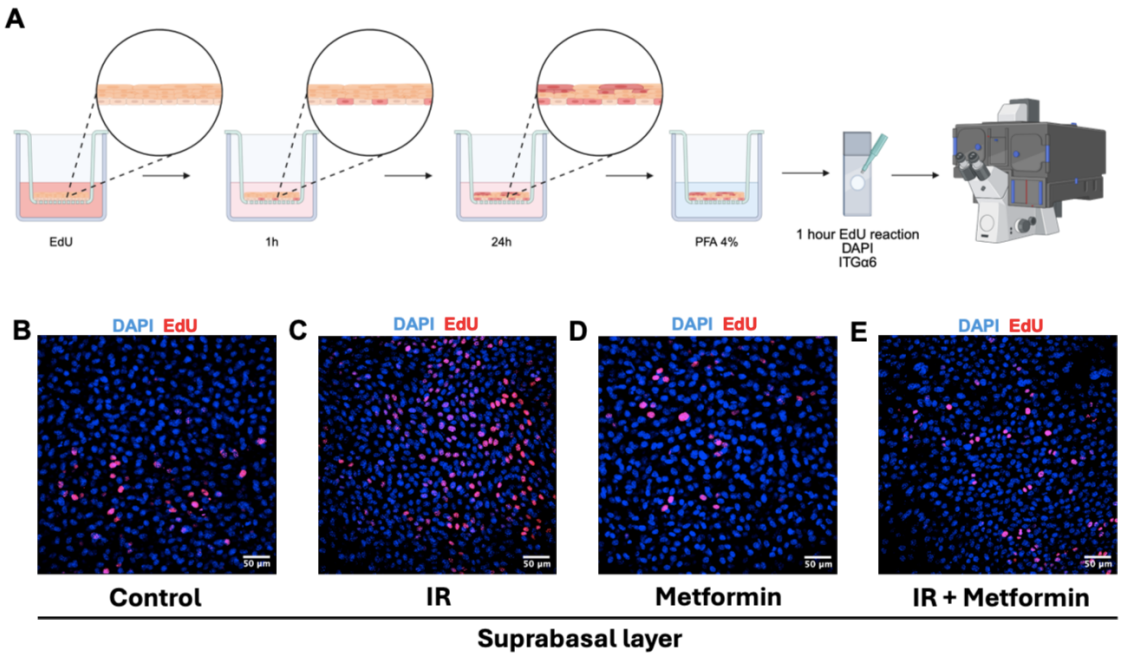

Figure 3. EdU differentiation tracing in mouse oesophageal epithelioids.

(A) Schematic cartoon representing how EdU staining works for tracing differentiation. It shows where EdU labelled cells (red) are located at different time points during EdU labelling. **(B-E)** Representative images from suprabasal layer cultures stained for DAPI (blue) and EdU (red). From B to E the four experimental groups are represented: CTRL, IR, Metformin and IR+Metformin. Schematic cartoon was made using BioRender.

Using p21 as a marker of senescence in mouse oesophageal epithelioids.

Senescence cells express p21 on their nuclei. Labelling p21 permits quantifying the number of senescence cells in a cell culture. With 3D oesophageal epithelium cultures, once they are fixed, p21 can be detected. In Figures 4A-D, basal layer is containing nuclei of active and proliferating cells (DAPI, blue), and it is also containing cells p21+. The proportion of these p21+ cells (or senescent cells) is less evident since these cultures have a huge number of cells constantly dividing and proliferating specially in the basal layer (as showed in Figures 3B-E).

Figures 4A-D represent the basal layer of 2.5 months-old mouse oesophagus cultures, where Figure 4A correspond to the control group, Figure 4B to the group exposed to radiation, Figure 4C to the metformin exposed group and Figure 4D to both radiation and metformin exposure. These figures can be correlated with Figure 4E, were comparing their p21+ quantification, show that there are no differences between groups.

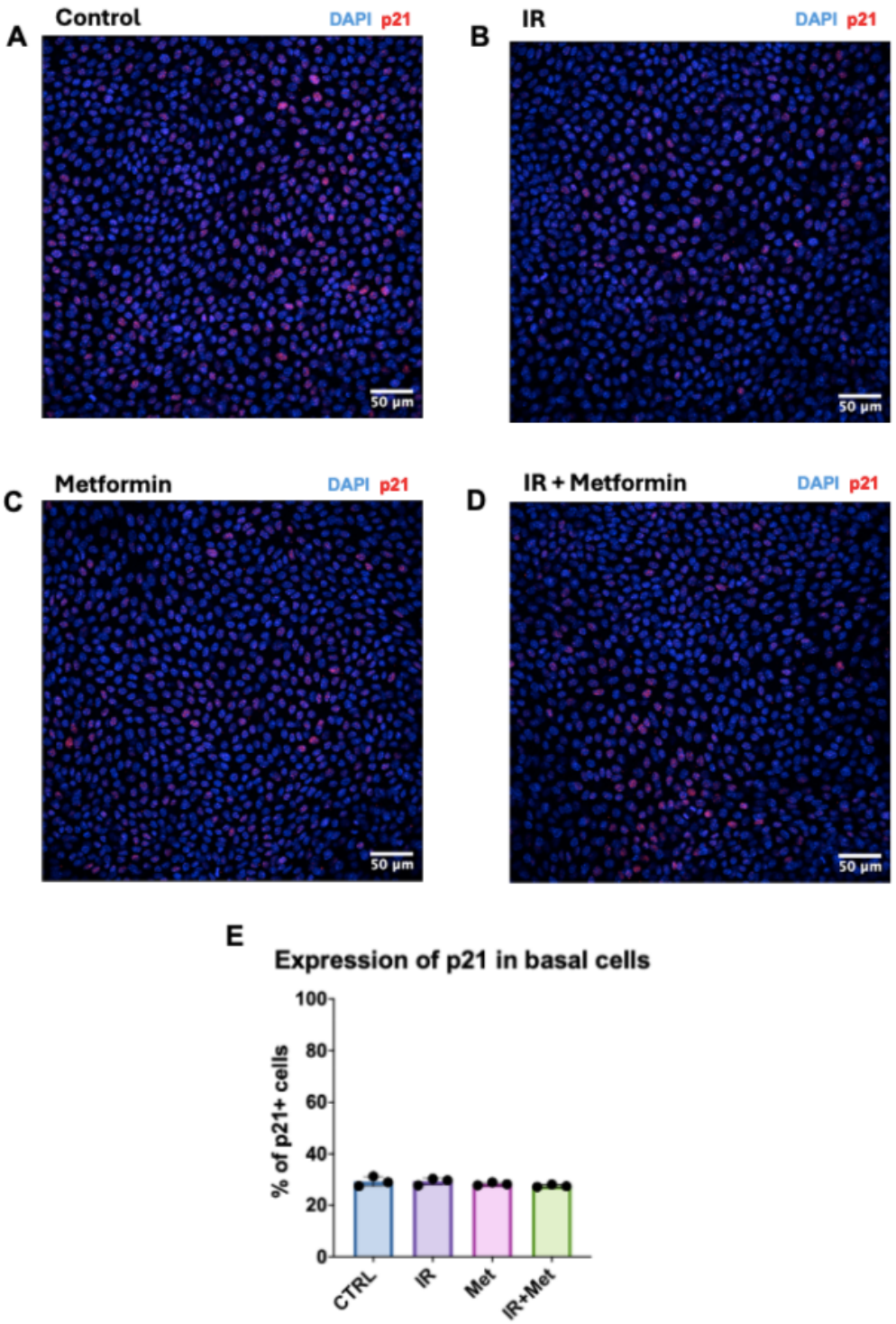

Figure 4. p21 expression in mouse oesophageal epithelioids.

(A-D) Representative images from suprabasal layer cultures stained for DAPI (blue) and p21 (red). From B to E the four experimental groups are represented: CTRL, IR, Metformin and IR+Metformin. **(E)** Graph showing the differences between the groups of cultured exposed to the different combinations of external factors. Y-axis represents percentage of basal cells expressing p21. Bars are the mean of the intensity on each group. Ordinary one-way ANOVA was the chosen statistical method n=3 different animals

DISCUSSION

While cell lines provide an excellent homogenous study material, 3D cultures models behave in a manner that is closer to the complex *in vivo* conditions[26,27]. 3D cultures have provided a method of choice for reconstructing tissues architecture and have developed a tool for better understanding changes, interactions and cellular and molecular signaling[28].

In the recent years, lots of types of 3D *in vitro* models have been generated. Depending on the specific objectives, models are usually carefully selected. By using scaffolds or Matrigel, extracellular matrix can be replicated using biocompatible materials. Cells are also allowed to maintain their properties, such as cell-cell and cell-matrix interactions, migration and intercellular signaling[28]. For instance, collagen I hydrogels cultured with human breast cancer. Collagen I biocompatibility allowed cells to proliferate without limitations, and the hydrogel architecture also facilitated interactions between cells and with the matrix[29]. Additionally, they are suitable for many applications, including cancer research, drug development, disease progression, regenerative medicine and stem cell research. Researchers developed in vitro culture systems with patient's peripherally and tumor-derived immune cells, which offered an approach to evaluate novel therapies in the context of heterogeneous tumor-associated cell types[30]. Microenvironmental immune cells can also be modelled in 3D systems[22]. Human diseases can also be modeled using organoids, such as steatohepatitis-like pathology generated from human induced pluripotent stem cells[31].

Despite their advantages, they present certain drawbacks. Although organotypic cultures and organoids provide tissue-like organization and amplification potential, they have no self-maintenance capacity and maximum experiment length without passaging is approximately one month. Some types of 3D cultures have specific material requirements for their maintenance and increased costs to produce them[24,28].

Long-term 3D epithelioids represent a versatile platform that provide new insights across diverse biological approaches and can have multiple applications. They allow generating 3D sheets of cultured primary epithelial tissue from small initial samples. A particular advantage of epithelioids over other 3D culture methods is they are capable to self-sustain for weeks to months without passaging, which offers a cost-effective approach to study long-term cellular processes. Epithelial 3D cultures also recapitulate the structure and architecture of mouse oesophageal epithelioids[24]. In the present study, it is demonstrated that 2.5 month-old mouse oesophageal epithelioids can replicate polarity, compartmentalization, and dynamics of mouse oesophageal epithelium. This was demonstrated by using different markers in both epithelioids and cryosections from mouse oesophagus. DAPI permitted identify cell localization and nuclear morphology, while polarity and tissue architecture were assessed using ITGα6 and phalloidin (an F-actin marker). Cell proliferation was analyzed by immunostaining for Ki67. Additionally, KLF4 was used as a differentiation marker. Suprabasal layers were labeled by immunostaining for keratin proteins such as KRT4 and KRT13, as well as loricrin for the upper layers.

Mouse oesophageal epithelioids were used in this experiment to model the effects of ageing. For that, external factors were employed to mimic ageing-related aspects. It is well documented that high dose of ionizing radiation has effects on radiation-induced ageing. However, evidence regarding the impact of low-dose radiation on ageing remains limited[11]. There are evidences that indicate that metformin has a clinical potential for ageing regulation and diseases control, since it acts promoting antioxidant

cell mechanisms[14]. To test both positive and negative effects that external factors can induce in cellular ageing, both radiation and metformin were used to test epithelioids as a model for ageing. The findings show that low dose radiation and metformin have effects on the cultures. Throughout the culture period, it was observed that metformin-treated cultures exhibited a faster color change in the medium, reflecting increased consumption. This phenomenon is linked to the mechanism of action of metformin, which inhibits the mitochondrial complex 1 of the electron transport chain, leading to a reduction in ATP levels that activates AMPK and also reduces the generation of reactive oxygen species (ROS)[13]. Additionally, increased number of shed cells was clear in radiation-exposed groups. Radiation induces differentiation, which reduces basal cell density and this triggers proliferation 24-48h later, associated with an accelerated turnover cells following radiation exposure[12]. The initial doses employed for the experiment were 0.5 mM metformin and 50 mGy ionizing radiation. Due to the lack of phenotypic changes at these concentrations, the doses were increased to 1 mM metformin and 100 mGy radiation.

Observations indicate that there is a strong correlation between the telomere shortening rate and the life span of a species[7]. Molecularly, to assess the effects of the external factors on the cultures, telomere length was measure by FISH. It was developed to assess it in histological sections to detect gradients of telomere length within tissues[32]. It was also used in paraffin-embedded adenopituitary tissue sections to compare telomere length between CDK4+ and CDK4- cells. This FISH technique was successfully applied in epithelioids, and the Cy3 fluorescence was acquired using confocal microscopy (*Methods*). However, care must be taken to preserve fixed tissues, avoiding using compounds that can interfere with cellular DNA, as this can compromise the results or cause this technique to fail.

It can be observed that radiation-exposed group had slightly lower intensity of signal comparing with control or metformin-exposed groups. Although a tendency was observed, those results did not present a statistical significance. Longer exposure to radiation or metformin together with extended time course experiments would be the key next step to further explore the suitability of this technique for assessment of the effects of longevity in epithelioids.

The same experiment was performed with cultures generated from a simple explant when compared to those generated from three explants. The results showed differences between both types of cultures. However, not statically difference was observed. Despite this, cultures generated from three explants confluence at a faster rate than the ones generated from a single explant. This suggests that cells from the second group replicated fewer times, which can correlate with higher preservation of telomere length. This finding highlights an opportunity to quantitatively assess the number of replication cycles required for cells to reach confluence. Implementing the use of cell trace markers in growing cultures would be interesting to perform in the future. It could provide valuable insight into the correlation between cellular replication and telomere dynamics, as well as improve understanding cells behavior in this type of 3D cultures.

5-ethynil 2´-deoxyuridine (EdU) labels progenitor cells from the basal layer in S phase of the cell cycle. These cells can keep dividing or decide to differentiate. It was observed that 24 hours after giving a pulse of radiation the proportion of EdU+ cells that differentiated (located in suprabasal layers) was higher in radiated cells than in control cells[12]. So those differentiating, moved towards the surface be becoming EdU+ supra

basal cells that carry the labelling from the basal layer, serving as a measure of cell differentiation in epithelioids.

EdU tracing can be correlated with cell density. It was previously shown that density of cells in the basal layer was reduced in irradiated mice and suprabasal cell density was increased[12]. In the present study, although not statically difference was observed, there is a tendence that shows that irradiated cultures have lower cell density compared to the other groups. Future experiments may quantify cell density and correlate it with proliferation and differentiation by quantifying EdU+ cells, to better understand how external factors can affect to epithelial cells.

Regarding p21 staining across the four experimental groups, no differences were found in the expression of this senescence markers in basal cells. Although metformin has effects in different cell pathways, some related to senescence, the expression of p21 is also regulated by multiple mechanisms[1].Therefore, expression of p21 alone may not provide definitive information about senescent cells in relation to metformin. On the other hand, there is evidence that senescence-associated markers are expressed consequently to radiation. Some of these represent late effects caused by therapeutic radiation treatments[33]. This suggest that senescence involves complex mechanisms, time- and dose- dependent, opening new research frontiers. The use of epithelioids can provide information in this regard, but longer culture periods and extended exposure times are needed to determine how external factors affect cell senescence and he mechanisms involved.

Correlation telomere length with the exposure to external factors (such as metformin and radiation) could yield deeper insights if telomeres length measurements are assessed at multiple time points throughout culture period. Extending this approach to include various tissue types epithelioids, including human epithelia (manual in preparation), may bring a closer understanding of the mechanisms involved in the ageing process.

In summary, the present study serves as a proof of concept that epithelioids can be used to investigate ageing-related biological processes *in vitro.* Their capacity to be maintained for long-term periods supports extended culture periods, increasing sampling, and studying how variations in the number of explants can affect proliferation and replication dynamics.

METHODS

Generation and maintenance of mouse oesophageal epithelioids.

Ethical permission for mouse experiments were done according to project license PP7037913. Animals were housed in individually ventilated cages and fed on standard chow. Mice were maintained at specific and opportunistic pathogen free health status.

Mice were euthanized and the oesophagus was removed with forceps. Then, the oesophagus was carefully opened using fine scissors. The oesophageal epithelium was separated from the submucosa and the muscle layer with fine tweezers. The oesophageal epithelium was cut with the scalpel into small pieces (1 mm^2 approximately). The explants obtained in the previous step were used to create the cultures. 3 explants were placed on top of a transparent ThinCert 0.4 µm pore-size six-well insert of 4.5 cm2 (Greiner Bio-One) with the epithelium facing upward.

Mouse oesophageal epithelioids were fed in complete FAD (cFAD) medium until confluence. This medium cFAD contains: Dulbecco's modified Eagle's medium/Nutrient Mixture F12 (DMEM/F12) at a ratio of 3:1 was made by mixing DMEM (Invitrogen, cat. no. 11971-025) and DMEM/F12 (Invitrogen, cat. no. 31330-038), supplemented with 5% fetal bovine serum (PAA Laboratories, cat. no. A15-041), 5% penicillin–streptomycin (Sigma-Aldrich, cat. no. P0781), 5 µg/ml insulin (Sigma-Aldrich, cat. no. I5500), 1.8 × 10^{-4} M adenine (Sigma-Aldrich, cat. no. A3159), 1 × 10^{-10} M cholera toxin (Sigma-Aldrich, cat. no. C8052), 10 ng/ml epidermal growth factor (PeproTech EC, cat. no. 100-15), 0.5 µg ml−1 hydrocortisone (Calbio-chem, cat. no. 386698) and 5 µg ml−1 apo-transferrin (Sigma-Aldrich, cat. no. T2036). Once the cultures are confluent, the medium is changed to minimum FAD (mFAD): DMEM (Invitrogen, cat. no. 11971-025) and DMEM/F12 (Invitrogen, cat. no. 31330-038) in a 1:1 ratio, supplemented with 5% fetal calf serum (PAA Laboratories, cat. no. A15-041), 5% penicillin–streptomycin (Sigma-Aldrich, cat. no. P0781), 5 µg ml−1 insulin (Sigma-Aldrich, cat. no. I5500) and 5 µg ml−1 apo-transferrin (Sigma-Aldrich, cat. no. T2036). Cultures were then always maintained in mFAD.

Immunostaining of mouse oesophageal epithelioids.

For epithelioid staining, inserts were first fixed in 4% paraformaldehyde (PFA) solution for 30 minutes at room temperature under gently shaking, followed by 3 washes with PHEM Buffer 1X (60 mM PIPES, 25 mM HEPES, 10 mM EGTA and 4 mM MgSO4·7H2O in PBS). Membranes were then separated from the inserts, and smaller biopsies were taken using 5mm diameter cutaneous biopsy punches (Kai industries; BP-50F). Membrane biopsies were permeabilized in PB Buffer (0.5% BSA, 0.25% fish skin gelatin, 1% Triton X-100 in PHEM) for 30 minutes at room temperature under gently shaking -all steps after this point were carried out under gentle shaking conditions-. Biopsies were then blocked in Blocking Buffer (PB Buffer + 10% Donkey serum) for 1 hour at room temperature. Biopsies were incubated with primary antibodies (Table S1) diluted in Blocking buffer overnight at room temperature, followed by 5 washes with PHEM buffer. After that, biopsies were incubated overnight with DAPI (1:1000), Phalloidin-A488 (1:1000) -when required- and secondary antibodies in Blocking buffer overnight at room temperature, followed by 5 washes with PHEM. Finally, Membrane biopsies were mounted in a 1:1 Glycerol-PBS solution on top of a glass slide and sealed with a thin coverslide.

Immunostaining of mouse oesophageal cryosections.

Small mouse oesophageal pieces were embedded in Optimal Cutting Temperature (OCT) solution, and frozen in dry ice. 10µmsectionswhere sliced using a cryostat (Leica CM3050 S) and placed on top Superfrost Microscopy slides (*VWR; 631-0909*). After that, slides were to air dried for 30 minutes and then fixed with PFA 4% for 5 minutes. OCT leftovers were removed by washing twice in PHEM buffer. Slides with the sections are blocked for 30 minutes in Blocking buffer (0.5% BSA, 0.25% fish skin gelatin, 0.5% Triton X-100 and 10% Donkey serum in PHEM) and then incubated inside a wet chamber with primary antibodies diluted in Blocking buffer overnight at room temperature. 5 to 10 washes with PHEM buffer were done after incubation with primary antibodies. Incubation with secondary antibodies in Blocking buffer with DAPI 1:1000 and Phalloidin 1:1000 was performed for 3 hours at room temperature. Finally, slides were mounted in a 1:1 Glycerol-PBS sealed by a glass coverslide.

Using low dose ionizing radiation and metformin in mouse oesophageal epithelioid cultures.

When cultures were confluent, medium was changed from cFAD to mFAD. Cultures were kept in mFAD for a week and then they were exposed to low dose ionizing radiation and/or metformin for 6 weeks.

Using a benchtop irradiator (Xstrahl; CIX1), 50 mGy pulses were given twice a week (every Monday and Thursday) to epithelioids for the first 4 weeks. After that, 100 mGy pulses were given twice a week (Monday and Thursday) during the final 2 weeks. In parallel, Metformin (LKT Laboratories) was administered the culture at a concentration of 0.5 mM for the first 2 weeks and increased to 1 mM for the subsequent 4 weeks. Medium was refreshed every 3-4 days, in synchrony with the exposure pulses, to maintain consistent drug exposure and nutrient availability.

FISH technique for quantification of telomer length in mouse oesophageal epithelioid cultures.

Small biopsies were first obtained using a 7mm cutaneous biopsy punch (Acu-punch®; P750). First, membrane biopsies were fixed in 4% PFA for 2 minutes and washed in 1X PBS for three times. All the washes were performed with PBS 1x unless otherwise indicated. Acidified pepsin (Pepsin 0.01% (w/v) in distilled water and pure hydrochloric acid 0.084% (v/v)) was used to incubate samples for 10 minutes at 37ºC to digest possible proteins that can be attached to the cellular DNA. Samples were again fixed with PFA 4% for 2 minutes and washed three times.

Membrane biopsies were then dehydrated in 5 minutes consecutive incubations of increasing ethanol concentrations (70%, 90%, 100%), followed by 20 minutes of air drying. Hybridation mix was prepared during incubations: TRIS 1M pH 7.4 (10 mM) + Hybridation buffer (Citric acid (15.3 µM), MgCl2 (42.5 µM), Na2HPO4 (139.4 µM)) + Formamide (70%) + SuperBlock buffer (5%) + Cy3-Tel (200 nM) in distilled water. Hybridation mix was added onto the punches mounted on slides and sealed with a glass coverslide slides were incubated in a hybridization oven for 5 minutes at 80 ºC. This step was followed by a 2-hours incubation in a wet, light-protected chamber.

Formamide buffer (70% formamide + TRIS 0.01M pH 7.4 + BSA 0.01% + destilled water) was used to wash the slides. Finally, epithelioid punches were washed with TBST buffer

(Tris-buffer saline 1x + Tween 20 0.08%) followed by PBS 1x prior to DAPI incubation for 30 minutes and mounting over microscopy slides in a 1:1 Glycerol-PBS solution and sealing with glass coverslides.

EdU tracing.

Prior to EdU incorporation, cultures were maintained in mFAD medium for 2 weeks. The final week, metformin was added to mFAD medium since cells habituate to those conditions. For EdU *in vitro* tracing, cultures were incubated in 10 μM EdU diluted in mFAD medium for 1 hour EdU solution was then removed and fresh mFAD was used to wash the cultures for 1 hour.24 hour chasing incubation time was left for cells to differentiate and migrate upwards. Finally, epithelioids were fixed in 4% PFA for 30 minutes at room temperature.

EdU fluorescence staining was performed using the Click-it kit (Invitrogen, #C10338) following manufacturer's instructions.

Confocal microscopy.

Images for characterisation and telomere length analysis were acquired using a Nikon CSU-W1 SoRa spinning disk confocal system equipped on a Nikon Ti2 microscope, controlled by NIS-Elements AR software (version 5.42.06). The system utilized a Prime 95B 1 camera. Samples were scanned using a Apo LWD 40x/1.15 water immersion objective. 3D z-stacks with a 0.3 μm between planes were imaged.

Images for EdU tracing and p21 staining were acquired using a Nikon AX R confocal microscope equipped on a Nikon Ti2 microscope, controlled by NIS-Elements AR software (version 5.42.06). Samples were scanned using a Apo LWD 40x/1.15 water immersion objective used was a 40X long working distance water immersion objective. Single plane or a 3D z-stack with 0.6 μm between planes were imaged for p21 and EdU respectively.

Data analysis.

3D-rendered and reconstructed orthogonal (XYZ) images were generated using Volocity v6.3.1 (Perkin Elmer). Representative images for telomere length measurement, EdU tracing and p21staining were analyzed using Fiji (ImageJ)[34]

A custom script was developed in collaboration with Richard Butler (Imaging analysis specialist, the Gurdon Institute Imaging facility) for Fiji[34] for high-throughput segmentation of DAPI labelled nuclei in 3D stacks and measure intensity in their telomere labelling. The script applies a 3D frequency bandpass filter with a standard deviation range of 2-10 μm. It then calculates a threshold to extract objects from the processed stack using Huang's fuzzy thresholding algorithm[35]. The detected objects are clustered using the OPTICS algorithm[36] to robustly join segmented components into 3D nuclei with a maximum reachability distance of 2.5 μm.

DSBDancer v0.8.2 plugin (previously developed in the Gurdon Institute Imaging Facility) for Fiji[34] was used to apply customisable, high-throughput pipelines for robust quantification of basal layer total nuclei and nuclear markers. Positive signal in nuclei with a radius range of 2.5-3 μm segmented by applying Otsu's method[37] to the frequency

filtered DAPI channel was quantified. Nuclei were scored as EdU positive if the Z-score for their mean EdU intensity was >= 0.8 standard deviations.

ACKNOWLEDGMENTS

I would like to thank the laboratory of David Fernández-Antorán for their support throughout all the months of my internship there, for their warm welcome, and for making me feel like one of the team from the very beginning. Thank you, David, for your trust and for allowing me to learn in the lab while enjoying every moment. Special thanks to Alberto, for teaching and guiding me from day one, and believing in my work.

I would also like to thank the Gurdon Institute in Cambridge for opening its doors to me, and to the entire team for their kindness and daily support. A special mention goes to Richard Butler, Image analysis specialist from the microscopy team for his collaboration developing a Plugin for the analysis performed in this work.

My deepest gratitude is always for my mother. Thank you, Mom, for everything- none of this would have been possible without your constant support and unconditional love.

REFERENCES

1. Li, Z., Zhang, Z., Ren, Y., Wang, Y., Fang, J., Yue, H., Ma, S., and Guan, F. (2021). Aging and age-related diseases: from mechanisms to therapeutic strategies. Biogerontology *22*, 165–187. https://doi.org/10.1007/s10522-021-09910-5.

2. López-Otín, C., Blasco, M.A., Partridge, L., Serrano, M., and Kroemer, G. (2023). Hallmarks of aging: An expanding universe. Cell *186*, 243–278. https://doi.org/10.1016/j.cell.2022.11.001.

3. Ogrodnik, M. (2021). Cellular aging beyond cellular senescence: Markers of senescence prior to cell cycle arrest in vitro and in vivo. Aging Cell *20*, e13338. https://doi.org/10.1111/acel.13338.

4. Blackburn, E.H., Epel, E.S., and Lin, J. (2015). Human telomere biology: A contributory and interactive factor in aging, disease risks, and protection. Science *350*, 1193–1198. https://doi.org/10.1126/science.aab3389.

5. Iskandar, M., Xiao Barbero, M., Jaber, M., Chen, R., Gomez-Guevara, R., Cruz, E., and Westerheide, S. (2025). A Review of Telomere Attrition in Cancer and Aging: Current Molecular Insights and Future Therapeutic Approaches. Cancers *17*, 257. https://doi.org/10.3390/cancers17020257.

6. Muñoz-Lorente, M.A., Cano-Martin, A.C., and Blasco, M.A. (2019). Mice with hyper-long telomeres show less metabolic aging and longer lifespans. Nat. Commun. *10*, 4723. https://doi.org/10.1038/s41467-019-12664-x.

7. Whittemore, K., Vera, E., Martínez-Nevado, E., Sanpera, C., and Blasco, M.A. (2019). Telomere shortening rate predicts species life span. Proc. Natl. Acad. Sci. U. S. A. *116*, 15122–15127. https://doi.org/10.1073/pnas.1902452116.

8. Stallaert, W., Kedziora, K.M., Taylor, C.D., Zikry, T.M., Ranek, J.S., Sobon, H.K., Taylor, S.R., Young, C.L., Cook, J.G., and Purvis, J.E. (2022). The structure of the human cell cycle. Cell Syst. *13*, 230-240.e3. https://doi.org/10.1016/j.cels.2021.10.007.

9. da Silva, P.F.L., and Schumacher, B. (2021). Principles of the Molecular and Cellular Mechanisms of Aging. J. Invest. Dermatol. *141*, 951–960. https://doi.org/10.1016/j.jid.2020.11.018.

10. Yan, J., Chen, S., Yi, Z., Zhao, R., Zhu, J., Ding, S., and Wu, J. (2024). The role of p21 in cellular senescence and aging-related diseases. Mol. Cells *47*, 100113. https://doi.org/10.1016/j.mocell.2024.100113.

11. Richardson, R.B. (2009). Ionizing radiation and aging: rejuvenating an old idea. Aging *1*, 887–902. https://doi.org/10.18632/aging.100081.

12. Fernandez-Antoran, D., Piedrafita, G., Murai, K., Ong, S.H., Herms, A., Frezza, C., and Jones, P.H. (2019). Outcompeting *p53*-Mutant Cells in the Normal Esophagus by Redox Manipulation. Cell Stem Cell *25*, 329-341.e6. https://doi.org/10.1016/j.stem.2019.06.011.

13. Mohammed, I., Hollenberg, M.D., Ding, H., and Triggle, C.R. (2021). A Critical Review of the Evidence That Metformin Is a Putative Anti-Aging Drug That Enhances Healthspan and Extends Lifespan. Front. Endocrinol. *12*, 718942. https://doi.org/10.3389/fendo.2021.718942.

14. Yang, Y., Lu, X., Liu, N., Ma, S., Zhang, H., Zhang, Z., Yang, K., Jiang, M., Zheng, Z., Qiao, Y., et al. (2024). Metformin decelerates aging clock in male monkeys. Cell *187*, 6358-6378.e29. https://doi.org/10.1016/j.cell.2024.08.021.

15. Duval, K., Grover, H., Han, L.-H., Mou, Y., Pegoraro, A.F., Fredberg, J., and Chen, Z. (2017). Modeling Physiological Events in 2D vs. 3D Cell Culture. Physiol. Bethesda Md *32*, 266–277. https://doi.org/10.1152/physiol.00036.2016.

16. Jensen, C., and Teng, Y. (2020). Is It Time to Start Transitioning From 2D to 3D Cell Culture? Front. Mol. Biosci. *7*, 33. https://doi.org/10.3389/fmolb.2020.00033.

17. Whelan, K.A., Muir, A.B., and Nakagawa, H. (2018). Esophageal 3D Culture Systems as Modeling Tools in Esophageal Epithelial Pathobiology and Personalized Medicine. Cell. Mol. Gastroenterol. Hepatol. *5*, 461–478. https://doi.org/10.1016/j.jcmgh.2018.01.011.

18. Urbani, L., Camilli, C., Phylactopoulos, D.-E., Crowley, C., Natarajan, D., Scottoni, F., Maghsoudlou, P., McCann, C.J., Pellegata, A.F., Urciuolo, A., et al. (2018). Multi-stage bioengineering of a layered oesophagus with in vitro expanded muscle and epithelial adult progenitors. Nat. Commun. *9*, 4286. https://doi.org/10.1038/s41467-018-06385-w.

19. Kalabis, J., Wong, G.S., Vega, M.E., Natsuizaka, M., Robertson, E.S., Herlyn, M., Nakagawa, H., and Rustgi, A.K. (2012). Isolation and characterization of mouse and human esophageal epithelial cells in 3D organotypic culture. Nat. Protoc. *7*, 235–246. https://doi.org/10.1038/nprot.2011.437.

20. Cesarz, Z., and Tamama, K. (2016). Spheroid Culture of Mesenchymal Stem Cells. Stem Cells Int. *2016*, 9176357. https://doi.org/10.1155/2016/9176357.

21. Kim, J., Koo, B.-K., and Knoblich, J.A. (2020). Human organoids: model systems for human biology and medicine. Nat. Rev. Mol. Cell Biol. *21*, 571–584. https://doi.org/10.1038/s41580-020-0259-3.

22. Neal, J.T., Li, X., Zhu, J., Giangarra, V., Grzeskowiak, C.L., Ju, J., Liu, I.H., Chiou, S.-H., Salahudeen, A.A., Smith, A.R., et al. (2018). Organoid Modeling of the Tumor Immune Microenvironment. Cell *175*, 1972-1988.e16. https://doi.org/10.1016/j.cell.2018.11.021.

23. Corrò, C., Novellasdemunt, L., and Li, V.S.W. (2020). A brief history of organoids. Am. J. Physiol. Cell Physiol. *319*, C151–C165. https://doi.org/10.1152/ajpcell.00120.2020.

24. Herms, A., Fernandez-Antoran, D., Alcolea, M.P., Kalogeropoulou, A., Banerjee, U., Piedrafita, G., Abby, E., Valverde-Lopez, J.A., Ferreira, I.S., Caseda, I., et al. (2024). Self-sustaining long-term 3D epithelioid cultures reveal drivers of clonal expansion in esophageal epithelium. Nat. Genet. *56*, 2158–2173. https://doi.org/10.1038/s41588-024-01875-8.

25. M, G.-L., V, Q., I, F., C, S., E, D.-R., Ma, J., Ak, R., Ma, B., C, D., M, M., et al. (2009). A GRFa2/Prop1/stem (GPS) cell niche in the pituitary. PloS One *4*. https://doi.org/10.1371/journal.pone.0004815.

26. Vinci, M., Gowan, S., Boxall, F., Patterson, L., Zimmermann, M., Court, W., Lomas, C., Mendiola, M., Hardisson, D., and Eccles, S.A. (2012). Advances in establishment and analysis of three-dimensional tumor spheroid-based functional assays for target validation and drug evaluation. BMC Biol. *10*, 29. https://doi.org/10.1186/1741-7007-10-29.

27. Ravi, M., Paramesh, V., Kaviya, S.R., Anuradha, E., and Solomon, F.D.P. (2015). 3D cell culture systems: advantages and applications. J. Cell. Physiol. *230*, 16–26. https://doi.org/10.1002/jcp.24683.

28. O, H., M, D.-A., F, C.-C., and L, D. (2021). 3D Cell Culture Systems: Tumor Application, Advantages, and Disadvantages. Int. J. Mol. Sci. *22*. https://doi.org/10.3390/ijms222212200.

29. Szot, C.S., Buchanan, C.F., Freeman, J.W., and Rylander, M.N. (2011). 3D in vitro bioengineered tumors based on collagen I hydrogels. Biomaterials *32*, 7905–7912. https://doi.org/10.1016/j.biomaterials.2011.07.001.

30. Finnberg, N.K., Gokare, P., Lev, A., Grivennikov, S.I., MacFarlane, A.W., Campbell, K.S., Winters, R.M., Kaputa, K., Farma, J.M., Abbas, A.E.-S., et al. (2017). Application of 3D tumoroid systems to define immune and cytotoxic therapeutic responses based on tumoroid and tissue slice culture molecular signatures. Oncotarget *8*, 66747–66757. https://doi.org/10.18632/oncotarget.19965.

31. Ouchi, R., Togo, S., Kimura, M., Shinozawa, T., Koido, M., Koike, H., Thompson, W., Karns, R.A., Mayhew, C.N., McGrath, P.S., et al. (2019). Modeling Steatohepatitis in Humans with Pluripotent Stem Cell-Derived Organoids. Cell Metab. *30*, 374-384.e6. https://doi.org/10.1016/j.cmet.2019.05.007.

32. Flores, I., Canela, A., Vera, E., Tejera, A., Cotsarelis, G., and Blasco, M.A. (2008). The longest telomeres: a general signature of adult stem cell compartments. Genes Dev. *22*, 654–667. https://doi.org/10.1101/gad.451008.

33. Kim, J.H., Brown, S.L., and Gordon, M.N. (2023). Radiation-induced senescence: therapeutic opportunities. Radiat. Oncol. Lond. Engl. *18*, 10. https://doi.org/10.1186/s13014-022-02184-2.

34. Schindelin, J., Arganda-Carreras, I., Frise, E., Kaynig, V., Longair, M., Pietzsch, T., Preibisch, S., Rueden, C., Saalfeld, S., Schmid, B., et al. (2012). Fiji: an open-source platform for biological-image analysis. Nat. Methods *9*, 676–682. https://doi.org/10.1038/nmeth.2019.

35. Huang, L.-K., and Wang, M.-J.J. (1995). Image thresholding by minimizing the measures of fuzziness. Pattern Recognit. *28*, 41–51. https://doi.org/10.1016/0031-3203(94)E0043-K.

36. Ankerst, M., Breunig, M.M., Kriegel, H.-P., and Sander, J. (1999). OPTICS: ordering points to identify the clustering structure. SIGMOD Rec *28*, 49–60. https://doi.org/10.1145/304181.304187.

37. Otsu, N. (1979). A Threshold Selection Method from Gray-Level Histograms. IEEE Trans. Syst. Man Cybern. *9*, 62–66. https://doi.org/10.1109/TSMC.1979.4310076.

Supplemental Information

In vitro modelling of ageing using long-term 3D epithelioids

Naiara Martínez Melgosa[1,2], Alberto Pradilla Dieste[2], David Fernández Antorán[2,3]

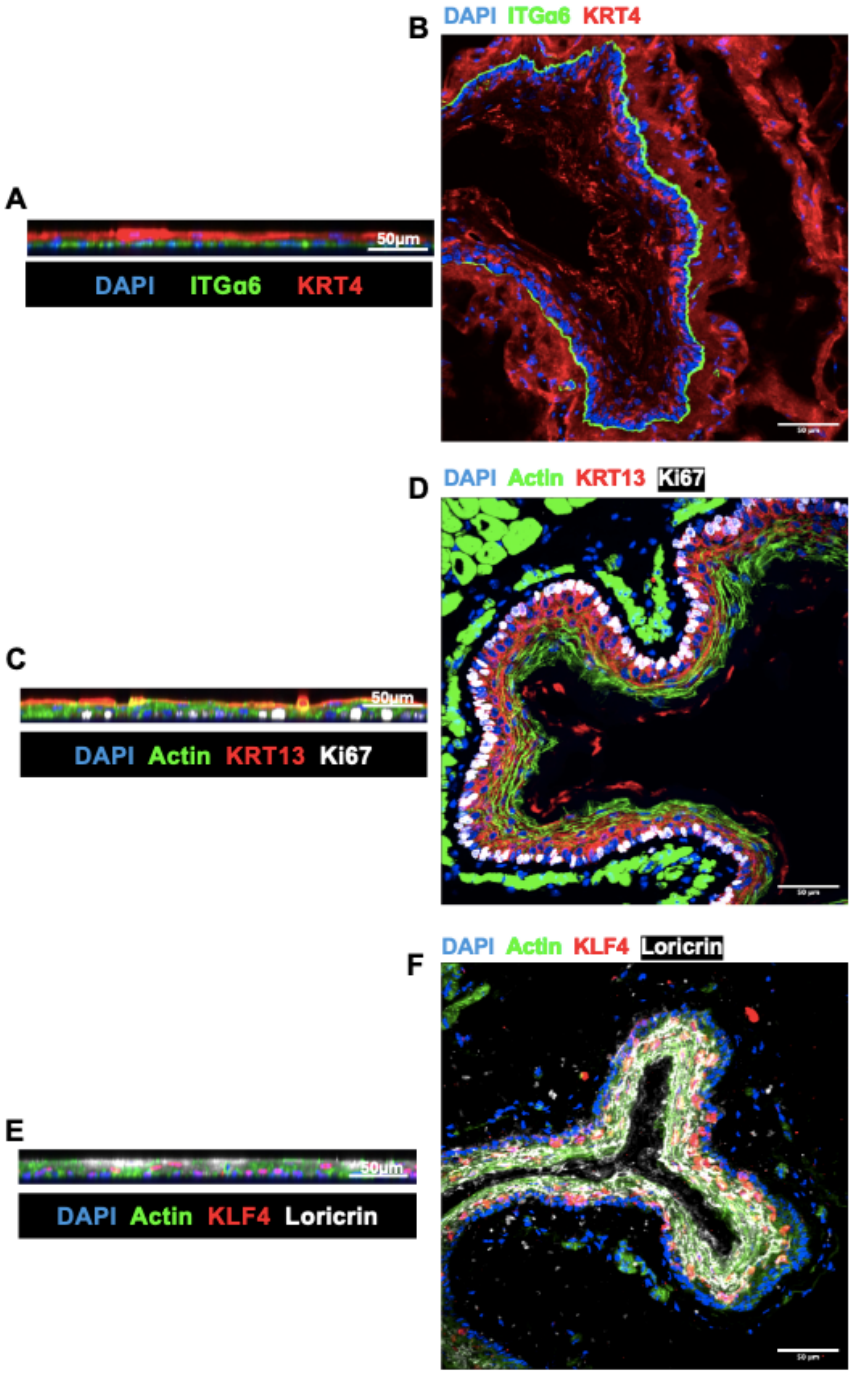

Figure S1. Comparison of mouse oesophageal epithelioid and mouse oesophagus architecture.

(A) Orthogonal view of mouse oesophageal epithelioid stained for DAPI (blue), ITGα6 (green) and KRT4 (red). **(B)** Mouse oesophageal cryosection stained for DAPI (blue), ITGα6 (green) and KRT4 (red). **(C)** Orthogonal view of mouse oesophageal epithelioid stained for DAPI (blue), Actin (green), KRT13 (red) and Ki67 (white). **(D)** Mouse oesophageal cryosection stained for DAPI (blue), Actin (green), KRT13 (red) and Ki67 (white). **(E)** Orthogonal view of mouse oesophageal epithelioid stained for DAPI (blue), Actin (green), KLF4 (red) and Loricrin (white). **(F)** Mouse oesophageal cryosection stained for DAPI (blue), Actin (green), KLF4 (red) and Loricrin (white).

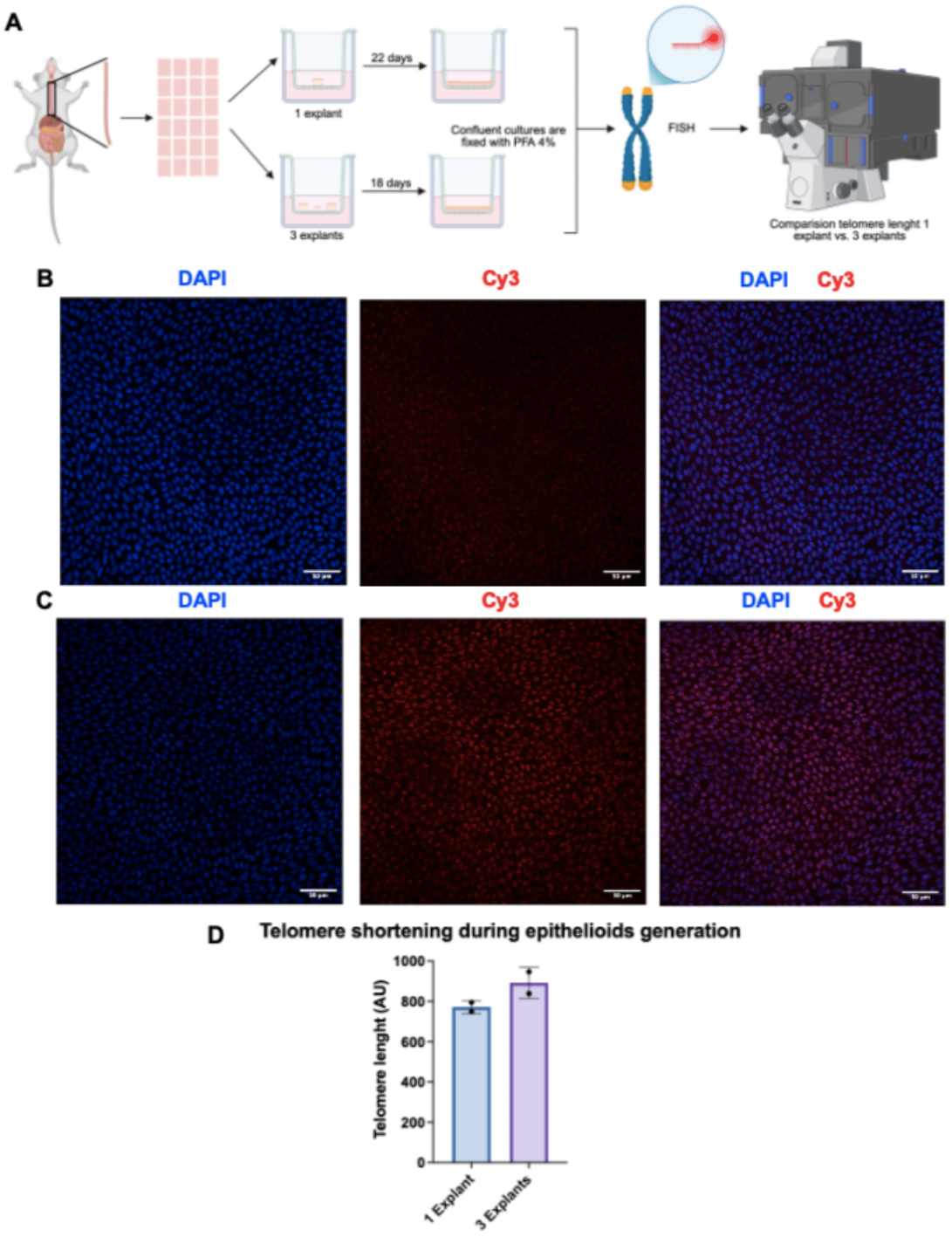

Figure S2. Differences in telomere shortening during epithelioids generation.

(A) Protocol for plating mouse oesophageal epithelium explants. **(B-C)** Representative images from basal layer cultures stained for DAPI (blue) and telomere C-rich repetitions (red). At the right, both DAPI (blue) and C-rich repetitions (red) are represented together. **(D)** Graph showing the differences between the cultures generated from one explant and the cultures generated from three explants. Y-axis represents the average of telomere length in intensity arbitrary units (AU). Bars represent the mean of the intensity on each group. Chosen statistical analysis was Ordinary one-way ANOVA. n=1 animal. Schematic cartoon was made using BioRender.

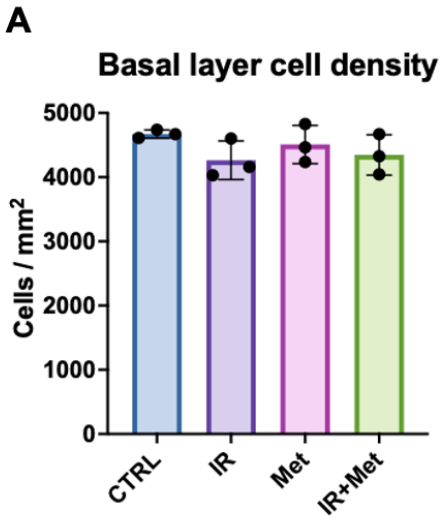

Figure S3. Basal layer cell density of 2.5 months-old mouse oesophageal epithelioids.

(A) Graph showing the differences between the density of nuclei detected in the basal layer of the four different groups of mouse oesophageal epithelioids. Y-axis represents the average of nuclei/cells per mm^2. Bars represent the mean of the cell density on each group. Chosen statistical analysis was Ordinary one-way ANOVA. n=3 animals.

Reagent or Resource

Primary antibody	Reference	Origin	Dilution
KRT4	Sigma-Aldrich; C5176	Mouse	1 in 500
KRT13	OriGene; BP5076	Guinea Pig	1 in 500
KI67	Abcam; ab 15580	Rabbit	1 in 900
KLF4	R&D Systems; AF3158	Goat	1 in 100
p21	BD Pharmingen; 556430	Mouse	1 in 300
Loricrin	Biolegend; B390970	Rabbit	1 in 500
ITGα6-647	Biolegend; B346058	Rat	1 in 500

Secondary antibody	Reference	Origin	Dilution
Anti-Mouse-A488 Plus	Invitrogen; A32766	Donkey	1 in 3000
Anti-Guinea pig-A647	Invitrogen; A21450	Goat	1 in 1000
Anti-Rabbit-A555 Plus	Invitrogen; A32794	Donkey	1 in 3000
Anti-Rabbit-A647 Plus	Invitrogen; A32795	Donkey	1 in 3000
Anti-Goat-A555 Plus	Invitrogen; A32816	Donkey	1 in 3000

Table S1. Antibodies used during the experiment.